TRACE SPECTRUM OF 1D TRANSFER MATRICES FOR WAVE PROPAGATION IN LAYERED MEDIA

J. GARCIA-SUAREZ

Abstract. The Transfer Matrix formalism is ubiquitous when considering wave propagation in various stratified media, applications ranging from Seismology to Quantum Mechanics. The relation between variables at two points in the laminate can be established via a matrix, termed (global) transfer matrix (product of "atomic" single-layer matrices). As a matter of convenience, we focus on 1D phononic structures, but our derivation can be extended to other fields where the formalism applies. We present exact expressions for entries of the global propagator for N layers. When the layering corresponds to a representative repeated cell in an otherwise infinitely periodic medium, the trace of the cumulative multi-layer matrix is known to control the dispersion relation. We show how this trace has a discrete spectrum made up of distinct 2^{N-1} harmonics (not necessarily orthogonal to each other in any sense) which we characterize exactly both in terms of the periods that they contain and their amplitudes; we also show that the phase shift among harmonics is either zero or π. This definite appraisal of the spectrum of the trace opens the path for rational design of band gaps, going beyond parametric or sensitivity studies.

1. Introduction

1.1. **Ubiquity of transfer matrix formalism.** The transfer matrix method, in its two-variable variant, refers to an approach to solve two coupled scalar linear 1st-order ODEs with two scalar unknowns, by instead of looking to combine equations into one, recasting them into a single vector linear 1st-order ODE, where the entries of the unknown vector correspond to the original scalar unknowns.

Let us mention some of the branches of Physics and Engineering where this method has been applied, along with some useful references (the following list is partial and does not intend to be thorough, the reader is invited to dive into the references included in the publications we make mention to in the ensuing).

- Electromagnetic waves [1]: working with frequency-domain 1D Maxwell equations, one can relate (a) the amplitude and (b) the spatial derivative of the amplitude along the propagation direction, of either the electric or the magnetic field, at any positions in a stratified medium with different dielectric constant in each layer (such a structure is usually referred as "photonic crystal"). In particular, in Optics, the numerical approach to working with these matrices is termed "Abeles Method" and it is used to obtain global properties of the layering, as, for instance, its reflectivity.
- Quantum Mechanics (Phononics): the time-independent 1D Schrodinger equation also admits a matrix representation [2], wherein the entries of the unknown vector are the wavefunction amplitude and its first derivative,

Date: June 2021.

the potential being discontinuous. The transfer matrix method induces a dynamic-system approach termed "trace maps" formalism [3]. Not only electronic properties affected by the stratification of the potential can be framed within this formalism, it also extends to lattice vibrations (phonons) and to quasi-periodic systems [4, 5].

- Acoustic waves: another field where the transfer matrix formalism finds natural applications is the design of acoustic metamaterials [6]: consider a periodic medium where pressure waves propagate, perpendicular to the interface between layers; then, the product of the successive transfer matrices, each one of them defined for a different layer, relate the pressure value at any two locations along the longitudinal coordinate. Thus, this matrix encodes the periodicity of a system (indeed, the Bloch condition is expressed in terms of the entries of the multi-layer transfer matrix).
- Elastic waves: (a) in Seismology [7, 8], the methodology is employed to study a number of scenarios of wave traversing across strata, from simple 1D wave propagation (geotechnical engineers would talk of "1D Site Response Analysis") to inclined P-SV waves. In the context of both Seismology and Geotechnical Earthquake Engineering, these matrices tend to be referred as "propagators", "propagator matrices" or "matrizants" in pioneer texts [9]. The goal of the analysis is, in most occasions, to relate the fields at a certain depth to the ones at the ground surface, after the waves traverse across a number of layers of different soils.
  (b) Laminates [10] are formally equivalent to the just mentioned soil strata. The main difference, despite formal similarities, is that one is also interested in understanding the effect of repeated layerings over the dispersion properties of the medium when assumed to be periodic. The study is tackled oftentimes in terms of either 1D compressional waves and shear waves. Cases other than propagation perpendicular to the layer edges have also been considered in the literature [11, 12].
  (c) Axial wave propagation in rods with changing cross-section and/or material properties is yet another category that can be considered [13, 14]. In general, also in this case, understanding the effect of periodic cells over the dispersion relation is the goal of the studies. See [15] for a recent review of applications of the method in mechanical engineering.

The latter configuration is the one we are to focus on in order to derive the new results, while some of our results may be generalizable to the other subjects which also employs the transfer matrix formalism in a different guise.

This wave propagation problem has received, and still receives, the attention of many researches in all the aforementioned fields. Hence it should not come as a surprise that the exact expression of the general (any number of layers) entries of the propagator matrix have been partially stated [16, 6], yet its general compact form is, to our knowledge, not available yet.

Moreover, in applications concerning elastic waves in laminates and rods, an elegant way of picturing the behavior of the dispersion relation by studying winding of a torus, whose surface represents the possible combinations of wavelengths in the laminate, was proposed recently in [17, 14]. This approach is "universal" insofar it permits to obtain some features of the dispersion relation for any kind of laminate or rod (e.g. the density of bandgaps). Remarkably, the aforementioned contributions

did not require the knowledge of the exact form of the global transfer matrix for any number of layers, but just the interpretation of the some arguments of the function controlling the dispersion relation as the flow over the toroidal surface.

When it comes to design questions, parametric and sensitivity studies have been favored [18, 19], owing to the apparent complexity of the entries of the global transfer matrix for any number of layers greater than two.

1.2. **Open questions in "bandgap engineering".** Assessing the influence of each design variable of the problem over, say, the dispersion relation of periodic structures is undoubtedly a challenge since the parameter space increases rapidly since every extra layer in the periodic cell introduces three independent parameters, in the particular case of periodic rods there are: length, cross-section area and material shear wave velocity. It is therefore not surprising that questions as the one we pass to pose have not received a general answer yet:

(1) Given a certain number of layers, what is the largest bandgap we can attain?
(2) How to combine material properties and layer thicknesses to achieve "optimal" (in some sense) bandgaps?
(3) Is the "optimal" design unique?
(4) Is there any benefit into having many layers instead of just a few? In other words, can one obtain a meaningful performance improvement that may justify a complexity increase (for instance, in terms of manufacturing cost)?

We do not intend to give closure to these matters in this paper, but we provide a new framework that can bring answers to them: we are to characterize the spectrum of the dispersion relation of a layered system. This enables a new approach to understanding both the behavior and the design of layered structures. The full potential of this tool has not been fully appraised yet, but we expect that future contributions will realize it.

1.3. **Structure of the text.** Section 2 presents the physical system under scrutiny as well as the equations governing it. Section 3 introduces the main result: the general expression of the trace of the cumulative transfer matrix over the characteristic cell of a periodic rod. This expression encodes the spectrum of the dispersion relation as a function of the geometric and material parameters. The section also includes verification of the result, while a detailed derivation has been consigned to the Appendix. Section 4 puts in display one logical manner of utilizing the newly-acquired knowledge of the spectrum to design a periodic rod whose first bandgap happens at the lowest possible frequency. Section 5 summarizes the main findings and lays out future directions in this field.

2. Preliminaries

2.1. **The system.** Figure 1 depicts the system: a representative cell made of N layers of different material and cross-sections, with thicknesses L_i, $i = 1, ..., N$, in an otherwise repetitive system assumed to be infinite.

The propagation of longitudinal waves in this system renders a 1D problem as the direction of propagation is perpendicular to all the interfaces between layers (and dispersive effects are not considered). The layer heterogeneity is described by the position-dependence in the cell of the Young's modulus, and the cross-section

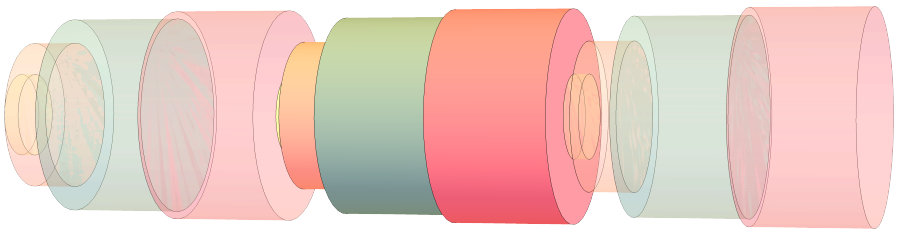

FIGURE 1. Scheme of the representative cell (highlighted) in a periodic rod to be subjected to axial wave propagation.

area. Material properties and the cross-section are assumed to remain constant in each layer.

2.2. **Governing equations.** In this scenario (rod axial waves, ignoring dispersive effects), the governing equations, in time domain, are

$$\frac{\partial}{\partial x}(\sigma A) = \rho \frac{\partial^2 u}{\partial t^2}\,, \tag{1a}$$

$$\frac{\partial u}{\partial x} = \frac{\sigma}{E}\,, \tag{1b}$$

where x is the longitudinal space coordinate, t represents time, σ is the normal stress to the interfaces, u is the longitudinal displacement, E is the Young modulus of the material the rod layer ("sub-rod") is made of, A is the cross-section area and ρ must be understood as a linear density, i.e., mass per unit of length. Either by taking the Fouier transform or by assuming a plane-wave *ansatz*, the frequency-domain version of these equations are

$$\frac{d}{dx}(\hat{\sigma} A) = -\rho \omega^2 \hat{u}\,, \tag{2a}$$

$$\frac{d\hat{u}}{dx} = \frac{\hat{\sigma}}{E}\,, \tag{2b}$$

where $\hat{u}$ and $\hat{\sigma}$ represent the amplitude of the displacement and the stress, respectively, and ω is the circular frequency. Recasting in matrix ODE form: for the k-th homogeneous portion [17],

$$\frac{d\boldsymbol{f}}{dx} = \frac{d}{dx}\begin{bmatrix}\hat{u}\\ \hat{\sigma}A\end{bmatrix} = \begin{bmatrix}0 & 1/a_k\\ -\rho_k\omega^2 & 0\end{bmatrix}\begin{bmatrix}\hat{u}\\ \hat{\sigma}A\end{bmatrix} = \boldsymbol{A}_k \boldsymbol{f}(z)\,,\,, \tag{3}$$

where $a_k = E_k A_k$. The solution, particularized at the end of the homogeneous sub-rod (whose length is L_k), is $\boldsymbol{f}(x_k) = \boldsymbol{T}_k(x_k, x_{k-1})\boldsymbol{f}(x_{k-1})$, where

$$\boldsymbol{T}_k(x_k, x_{k-1}) = \exp\left(L_k \boldsymbol{A}_k\right) = \begin{bmatrix}\cos\left(\frac{\omega L_k}{c_k}\right) & \frac{\sin\left(\frac{\omega L_k}{c_k}\right)}{\sqrt{\rho_k a_k}}\\ -\sqrt{\rho_k a_k}\,\sin\left(\frac{\omega L_k}{c_k}\right) & \cos\left(\frac{\omega L_k}{c_k}\right)\end{bmatrix}\,, \tag{4}$$

where $c_k = \sqrt{a_k/\rho_k}$.

By recursion, the motion-stress vector at any position in the cell (say, somewhere within the k-th layer) can be written in terms of the one at the initial point ($x = x_0$),

in particular to the end of the N-th layer, x_N:

(5)
$$\boldsymbol{f}(x_N) = \boldsymbol{T}(x_N, x_0)\boldsymbol{f}(x_0) = \boldsymbol{T}_N(x_N, x_{N-1}) \dots T_k(x_k, x_{k-1}) \dots T_1(x_1, x_0)\boldsymbol{f}(x_0)\,.$$

One further advantage of this method is that it ensures continuity of both displacements and tractions at every interface.

2.3. **Group-theoretical Aspects.** It has already been noted elsewhere [4] that the transfer matrices represent elements of the special linear group $SL(2,\mathbb{R})$ [20].

The group $SL(2,\mathbb{R})$ is related to the Lorentz-like group $SO(2,1)$ [21], what allows to regard the propagator matrices as Lorentz-transformation in 2D space, namely, the so-called "rapidity boosts".

This kind of group isomorphism belongs in the category termed "accidental" or "exceptional", as they arise as a consequence of the low-dimensionality of the ambient space being considered (two-by-two matrices), not from a genuine connection between groups that persists in higher dimensions. These equivalences can be exploited nonetheless, and we will leverage the isomorphism $SO(2,1)$ to derive exact expressions of the cumulative propagator, see the Appendix.

2.4. **Periodicity and dispersion relations.** Bloch condition [22] demands that $\boldsymbol{f}(x = L) = \boldsymbol{T}(L, 0)\boldsymbol{f}(x = 0) = \exp(\mathrm{i}\mathrm{k}L)\boldsymbol{f}(0)$ in the periodic medium, k being the wavenumber.

For the relation to have non-trivial solutions, $\exp(\mathrm{i}\mathrm{k}L)$ must be an eigenvalue of $\boldsymbol{T}(L, 0)$. The equation for the eigenvalues, λ, is

$$\lambda^2 - \mathrm{trace}(\boldsymbol{T}(L, 0))\lambda + 1 = 0\,, \tag{6}$$

where the fact that $\det \boldsymbol{T}(L, 0) = T_{22}T_{11} - T_{21}T_{12} = 1$ (it is a matrix of the special linear group, after all) has been used. Substituting $\lambda = \exp(\mathrm{i}\mathrm{k}L)$ in eq. (6), and then multiplying by $\exp(-\mathrm{i}\mathrm{k}L)$, gathering terms, yields

$$\cos(\mathrm{k}L) = \frac{1}{2}\mathrm{trace}(\boldsymbol{T}(L, 0))\,. \tag{7}$$

See that for as long as $|\mathrm{trace}(\boldsymbol{T}(L, 0))| \leq 2$, the prior transcendental equation admits real wavenumbers as solutions, so waves propagate at those frequencies, but if $|\mathrm{trace}(\boldsymbol{T}(L, 0))| > 2$, the solution implies imaginary wavenumbers, thus the waves must decay in amplitude exponentially: in other words, no propagation occurs, there would be a bandgap at that frequency.

3. The trace exact formula

The general recursion yields the following expression for the half-trace:

$$\frac{1}{2}\mathrm{trace}(\boldsymbol{T}(L, 0)) = \frac{T_{11} + T_{22}}{2} = \left(\prod_{i=1}^{N} \cos(r_i)\right)\left(1 - \sum_{\beta=1}^{\lfloor N/2 \rfloor} \sum_{|\mathsf{b}|=2\beta} C_{\mathsf{b}} \tan(r)^{\mathsf{b}}\right)\,, \tag{8}$$

each $\mathsf{b} \in (\{0,1\})^N$ is a multi-index [23] representing one permutation out of $\binom{N}{2\beta}$ possible ones having $|\mathsf{b}| = 2\beta$ terms equal to one while the other ones are zero, the coefficients C_{b} being given by

$$C_{\mathsf{b}} = \frac{(-1)^{|\mathsf{b}|/2}}{2}\left[(\sqrt{\rho a})^{\mathrm{f}(\mathsf{b})} + (\sqrt{\rho a})^{-\mathrm{f}(\mathsf{b})}\right]\,. \tag{9}$$

where the map $\mathrm{f}:(\{0,1\})^N \to (\{-1,0,1\})^N$ takes the multi-index b, entry-wise, to the multi-index $\mathrm{f}(\mathsf{b})$ defined as:

- if $\mathsf{b}_i = 0$, then $\mathrm{f}(\mathsf{b}_i) = 0$,
- if $\mathsf{b}_i = 1$ and the previous value assigned by f to the prior 1-entry in b was -1, then $\mathrm{f}(\mathsf{b}_i) = 1$, else $\mathrm{f}(\mathsf{b}_i) = -1$.

Through this auxiliary multi-index $\mathrm{f}(\mathsf{b})$ the impedance contrasts enter the results.

The design example in Section 4 outlines how the multi-indices are constructed and how in turn they define the half-trace function. The first addends, those that go with $\mathrm{f}(\mathsf{b})$, correspond to T_{11} while T_{22} provides those with $-\mathrm{f}(\mathsf{b})$ see Appendix.

The total number of addends in the sum in the previous expressions is equal to

$$N_{addends} = \binom{N}{2} + \binom{N}{4} + \ldots + \binom{N}{\lfloor N/2 \rfloor} = \sum_{k=1}^{\frac{1}{2}\lfloor N/2 \rfloor} \binom{N}{2k} = 2^{N-1} - 1\,. \tag{10}$$

Resorting to the product-to-sum identity, the right-hand side of Equation (8) can be converted into a sum of 2^N products, each one of them being a product of N functions, either sines or cosines. The identity states:

$$\prod_{i=1}^{N} \cos(\theta_i) = \frac{1}{2^N} \sum_{\mathsf{e}\in(\{-1,1\})^N} \cos\left(\sum_{j=1}^{N} \mathsf{e}_j \theta_j\right)\,, \tag{11}$$

for any arguments θ_i, $i = 1, \ldots, N$.

Since all the sines that appear can be considered as cosines with extra phase $-\pi/2$, they would also fit in the identity. Even more remarkable is the fact that, given that the degree of the multi-index $\mathsf{b}$is always even, these sine terms (regarded as out-of-phase cosines) entail either a change of sign or nothing at all, so the final result will be a sum of cosine functions without phase-delay terms.

Summarizing, the half-trace function in Equation (8) admits the following form

$$\frac{1}{2}\mathrm{trace}(\boldsymbol{T}(L,0)) = \sum_{k=1}^{2^N} \mathcal{T}_k \cos\left(\tau_k \omega\right)\,, \tag{12}$$

where the discrete spectrum of the half-trace of the laminate is fully defined by the characteristic "spectral periods" of the N-layer periodic cell, given by

$$\tau_k = \sum_{j=1}^{N} \mathsf{e}_{kj} L_k / c_k\,, \tag{13a}$$

and its corresponding "spectral amplitudes"

$$\mathcal{T}_k = \sum_{\mathsf{b}} \frac{(-1)^{\mathsf{b}\cdot\mathsf{e}_k/2}}{2^N} C_{\mathsf{b}}\,, \tag{13b}$$

where the coefficient C_{b} (made up of contribution of impedance contrasts) associated to each multi-index b was defined in Equation (9), and the exponent of -1, controlling the overall sign of each addend, represents the inner product of two multi-indices as if they were vectors. See that the amplitudes must meet the following condition:

$$\sum_{k=1}^{2^N} \mathcal{T}_k = 1\,, \tag{14}$$

note that eq. (13a) could also be expressed in terms of ratios of length over wavelength in the material, if we took the material of each layer to be given and its length to remain changeable.

In light of eq. (6), we can say that eq. (12) defines the spectrum for any variable-cross-section modular rod, and for any periodic laminate for that matter.

3.1. **Verifications.** Before proceeding to evaluate the analytical result, compare it to the direct evaluation of the transfer matrices and analyze the spectrum, we can apply the symmetry of the cosine, i.e. the fact that $\cos(x) = \cos(-x)$, to see that the previous identity would give us a symmetric two-sided spectrum, which can be reduced to a one-sided spectrum retaining the same information. This is achieved by fixing $\mathsf{e}_1 = 1$ in all cases and leaving free the other components $(\mathsf{e}_2 \ \ldots \ \mathsf{e}_N) \in (\{1, 0, -1\})^{N-1}$; this modified multi-index is referred as $\tilde{\mathsf{e}}$:

$$\prod_{i=1}^{N} \cos(\theta_i) = \frac{1}{2^{N-1}} \sum_{\tilde{\mathsf{e}}} \cos\left(\sum_{j=1}^{N} \tilde{\mathsf{e}}_j \theta_j \right) . \tag{15}$$

In order to verify eq. (12), we study 10 cases with different cross-sections and materials in the unit cell. These 10 cases are borrowed from previous work by Kaklamanos and colleagues [24] who used 10 Kiknet [25] profiles to analyze the transfer function in layered sites; we adapt the physical quantities to represent rod properties instead of geotechnical info.

We compare the solution provided by the analytical solution to the one obtained from multiplying propagating matrices (following the numerical implementation described in [7]). Find in the following pages the images of three representative scenarios, the rest can be found in the appendix.

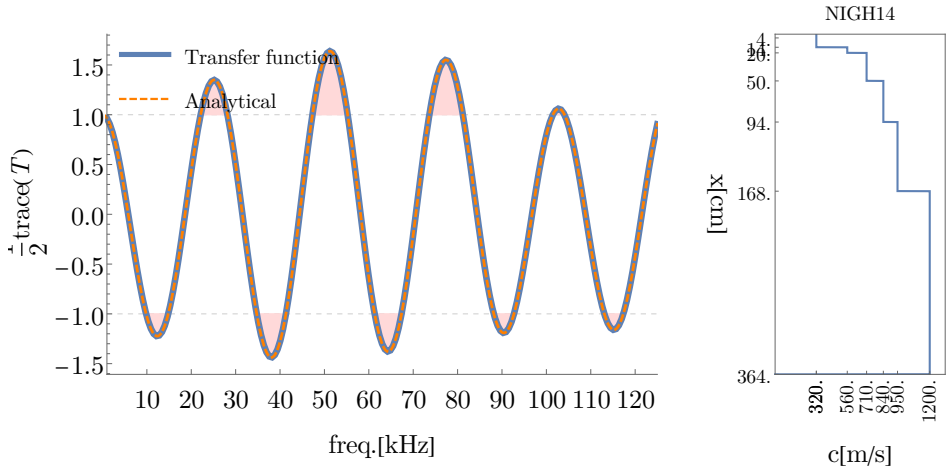

FIGURE 2. Dispersion diagram (left panel) and spectrum of half-trace (right panel) of rod having properties (right panel) that mirror Kik-Net site NIGH14 (shaded region in left panel corresponds to bandgap).

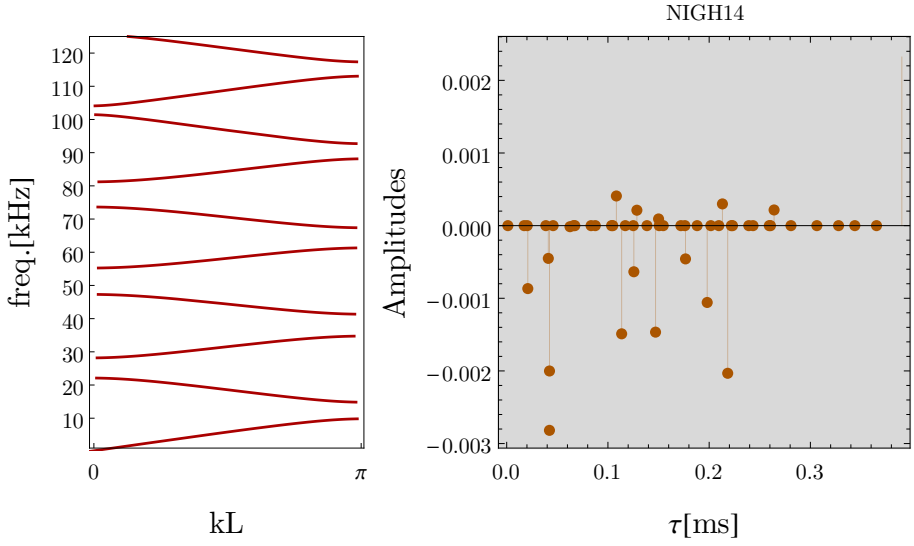

FIGURE 3. Dispersion diagram (left panel) and spectrum of half-trace (right panel) of rod having properties (right panel) that mirror Kik-Net site NIGH14.

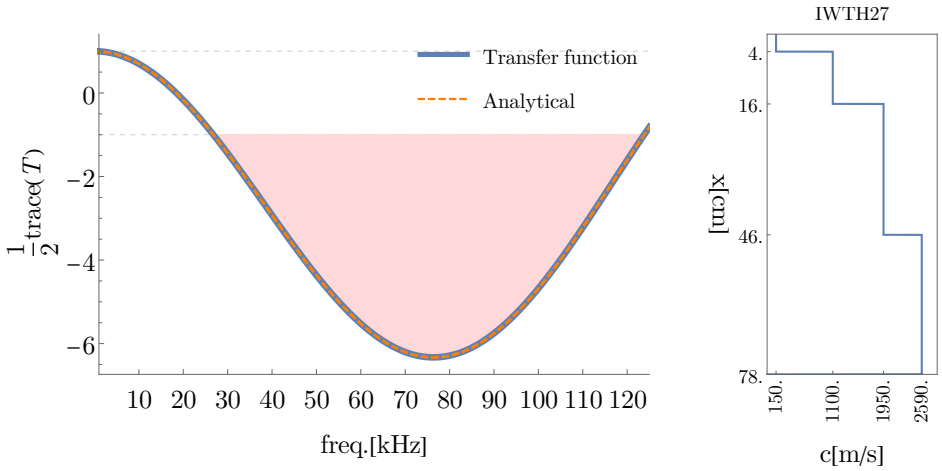

FIGURE 4. Dispersion diagram (left panel) and spectrum of half-trace (right panel) of rod having properties (right panel) that mirror Kik-Net site IWTH27 (shaded region in left panel corresponds to bandgap).

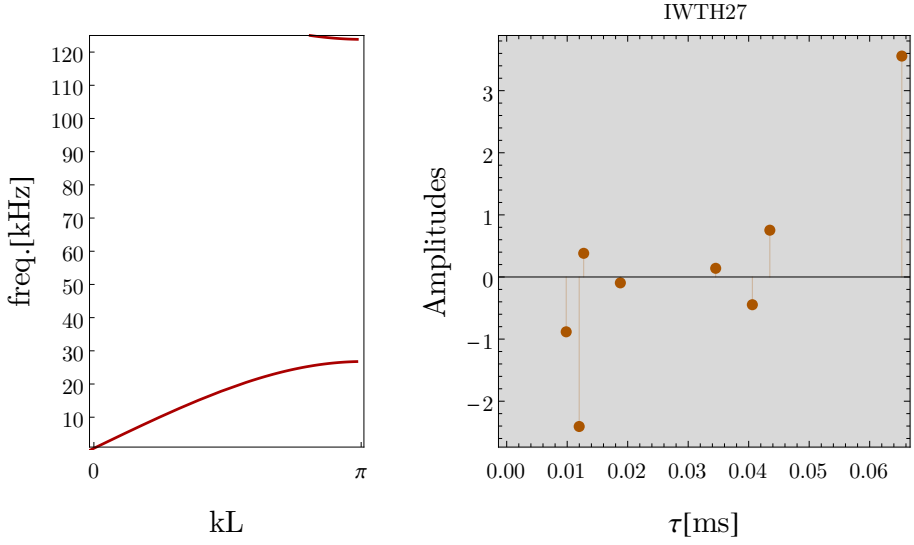

FIGURE 5. Dispersion diagram (left panel) and spectrum of half-trace (right panel) of rod having properties (right panel) that mirror Kik-Net site IWTH27.

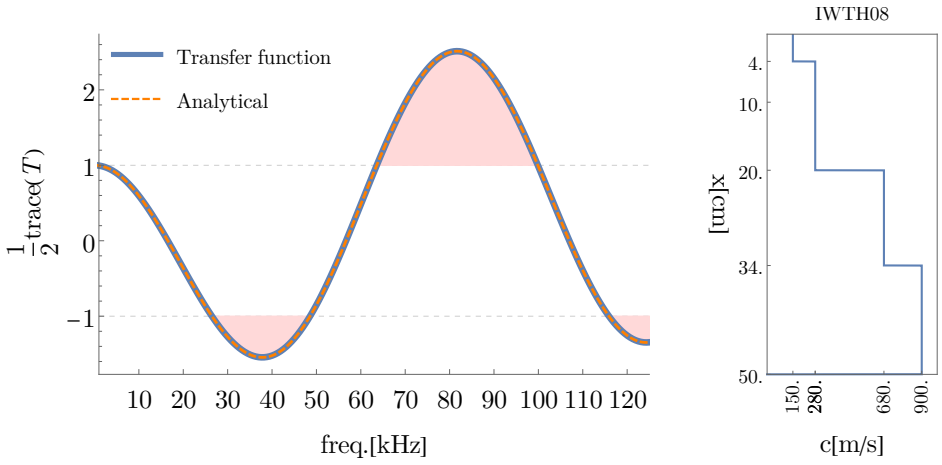

FIGURE 6. Dispersion diagram (left panel) and spectrum of half-trace (right panel) of rod having properties (right panel) that mirror Kik-Net site IWTH08 (shaded region in left panel corresponds to bandgap).

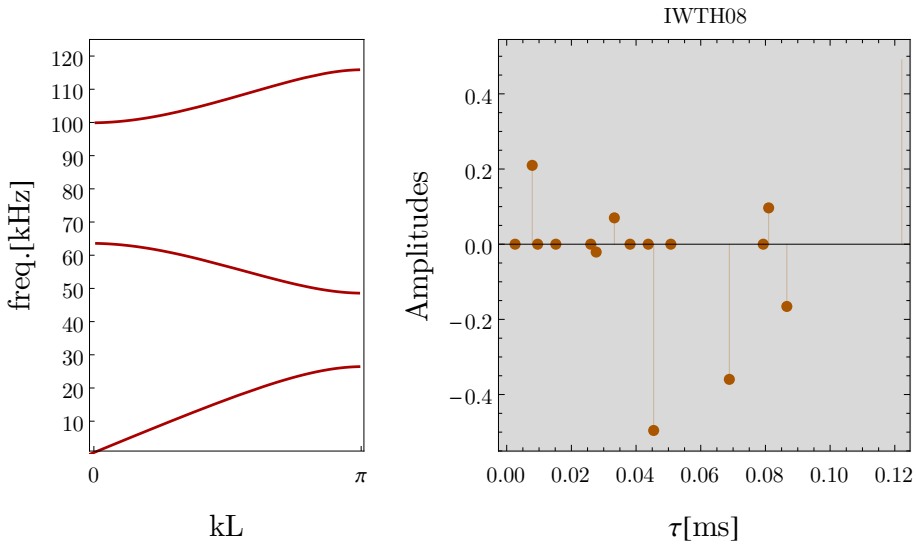

FIGURE 7. Dispersion diagram (left panel) and spectrum of half-trace (right panel) of rod having properties (right panel) that mirror Kik-Net site IWTH08.

Let us discuss the previous results briefly:

- Figure 2 and Figure 3 show a system, made up of 7 layers that presents many small bandgaps, as the half-trace function surpasses ± 1 over a number of small intervals. In this case there are $2^6 = 64$ harmonics in the one-sided spectrum, which can be seen to be very small amplitude (~ 0.001) is most cases, see Figure 3, thus the corresponding oscillations do not sum up much over unity thus the bandgaps are many (so there is much oscillations) and small in width.
- Figure 4 and Figure 5, conversely, shows quite the opposite situation: there are 4 layers, hence only $2^3 = 8$ harmonics, and there are two of them whose amplitude is well above the rest (greater than 2 actually), one at the beginning and the other at the end of the spectrum, see Figure 5. See that these two harmonics are "spectrally separated", one of them can be considered as a quick variable and the other one as a slow one, so they do not balk each other.
- Figure 6 and Figure 7 displays an intermediate scenario: there are a few harmonics, out of $2^4 = 16$, that have tiny amplitude, while the rest do not have much, none of them above 0.5 in absolute value (greater than those in the first case, ~ 0.001, yet smaller than the ones in the second case, ~ 1). Greater amplitudes are attained at the middle of the spectrum, see Figure 7, while .

4. Leveraging spectral properties of the trace for design purposes: widening the first gap in a 3-layer system

One obvious way to attain a large magnitude of the half-trace function for as low a frequency as possible, and hence a wide bandwidth at low frequency, is to maximize the amplitude of the"quickest" harmonic (the one where the permutation signs are all positive), i.e. $r_1 + r_2 + r_3 = \tau_1\omega = (h_1/c_1 + h_2/c_2 + h_3/c_3)\omega$. The apparent issue with this approach is that the gap will not be as wide as if it relied on the "slower" variables.

Let us take advantage of this exercise to illustrate how the trace can be constructed using the combinatorics encoded in the multi-index with no appeal whatsoever to any transfer matrix, just following the combinatorial rules for the multi-indices outlined before. We also introduce the inter-layer impedance contrast $Z_i = \sqrt{\rho_i a_i}/\sqrt{\rho_{i+1} a_{i+1}}$, a parameter that allows to render the results in compact form. In this case, $N = 3$, we have the following possible b values, which are mapped by f as

$$\mathsf{b} = (1,1,0) \to \mathrm{f}(\mathsf{b}) = (1,-1,0) \to \frac{\sqrt{\rho_1 a_1}}{\sqrt{\rho_2 a_2}} = Z_1\,, \tag{16a}$$

$$\mathsf{b} = (1,0,1) \to \mathrm{f}(\mathsf{b}) = (1,0,-1). \to \frac{\sqrt{\rho_1 a_1}}{\sqrt{\rho_3 a_3}} = Z_1 Z_2\,, \tag{16b}$$

$$\mathsf{b} = (0,1,1) \to \mathrm{f}(\mathsf{b}) = (0,1,-1) \to \frac{\sqrt{\rho_2 a_2}}{\sqrt{\rho_3 a_3}} = Z_2\,, \tag{16c}$$

likewise, the multi-index $\tilde{\mathsf{e}} \in (\{-1,1\})^N$ yields the periods, and also the amplitudes in tandem with the corresponding f(b):

$$\text{(17a)}\quad \tilde{\mathsf{e}} = (1,1,1) \to \tau_1 = \frac{L_1}{c_1} + \frac{L_2}{c_2} + \frac{L_3}{c_3} \text{ and } \mathcal{T}_1 = 1 + \tfrac{1}{2}Z_1 + \tfrac{1}{2}Z_1Z_2 + \tfrac{1}{2}Z_2\,,$$

$$\text{(17b)}\quad \tilde{\mathsf{e}} = (1,-1,1) \to \tau_2 = \frac{L_1}{c_1} - \frac{L_2}{c_2} + \frac{L_3}{c_3} \text{ and } \mathcal{T}_2 = 1 - \tfrac{1}{2}Z_1 + \tfrac{1}{2}Z_1Z_2 - \tfrac{1}{2}Z_2\,,$$

$$\text{(17c)}\quad \tilde{\mathsf{e}} = (1,1,-1) \to \tau_3 = \frac{L_1}{c_1} + \frac{L_2}{c_2} - \frac{L_3}{c_3} \text{ and } \mathcal{T}_3 = 1 + \tfrac{1}{2}Z_1 - \tfrac{1}{2}Z_1Z_2 - \tfrac{1}{2}Z_2\,,$$

$$\text{(17d)}\quad \tilde{\mathsf{e}} = (1,-1,-1) \to \tau_4 = \frac{L_1}{c_1} - \frac{L_2}{c_2} - \frac{L_3}{c_3} \text{ and } \mathcal{T}_4 = 1 - \tfrac{1}{2}Z_1 - \tfrac{1}{2}Z_1Z_2 + \tfrac{1}{2}Z_2\,,$$

see how indeed we have $\mathcal{T}_1 + \mathcal{T}_2 + \mathcal{T}_3 + \mathcal{T}_4 = 1$. If the first harmonic oscillates much faster than the others, it will cause the half-trace to go well beyond 1 before the overall amplitude is affected by the other oscillatory terms. The amplitude of this harmonic is given by $\mathcal{T}_1 = 1 + Z_1 + Z_1Z_2 + Z_2$.

Therefore, let us re-state the design problem as maximizing simultaneously $\mathcal{T}_1$ and τ_1, the latter with respect to all the others τ_i for all $i > 1$.

Moreover, in this case, one can make the potentially-slowest harmonic, the one corresponding to $r_1 - r_2 - r_3 = \omega(L_1/c_1 - L_2/c_2 - L_3/c_3)$, not to oscillate at all if lengths and velocities are chosen such that $(L_1/c_1 - L_2/c_2 - L_3/c_3) \approx 0$. If the corresponding amplitude is negative, it would mean that its effect reinforces the bandgap generated by the oscillation of the quick harmonic.
Finally, the two intermediate harmonics can be made to cross zero (and add no amplitude in either way) at the same time that the quick harmonic reaches its first peak, by sensibly choosing the relation between lengths and wave velocity.

For the sake of clarity, let us show in all detail how the global half-trace looks like:

$$\begin{aligned}
\frac{1}{2}\tan(\boldsymbol{T}(0,L)) =& \tfrac{1}{4}\left(1 + \tfrac{1}{2}\frac{\sqrt{\rho_1 a_1}}{\sqrt{\rho_2 a_2}} + \tfrac{1}{2}\frac{\sqrt{\rho_1 a_1}}{\sqrt{\rho_3 a_3}} + \tfrac{1}{2}\frac{\sqrt{\rho_2 a_2}}{\sqrt{\rho_3 a_3}}\right) \\
&\qquad \cos\left(\left[\frac{L_1}{c_1} + \frac{L_2}{c_2} + \frac{L_3}{c_3}\right]\omega\right) \textit{(first harmonic)} \\
&+ \tfrac{1}{4}\left(1 - \tfrac{1}{2}\frac{\sqrt{\rho_1 a_1}}{\sqrt{\rho_2 a_2}} + \tfrac{1}{2}\frac{\sqrt{\rho_1 a_1}}{\sqrt{\rho_3 a_3}} - \tfrac{1}{2}\frac{\sqrt{\rho_2 a_2}}{\sqrt{\rho_3 a_3}}\right) \\
&\qquad \cos\left(\left[\frac{L_1}{c_1} - \frac{L_2}{c_2} + \frac{L_3}{c_3}\right]\omega\right) \textit{(second harmonic)} \\
&+ \tfrac{1}{4}\left(1 + \tfrac{1}{2}\frac{\sqrt{\rho_1 a_1}}{\sqrt{\rho_2 a_2}} - \tfrac{1}{2}\frac{\sqrt{\rho_1 a_1}}{\sqrt{\rho_3 a_3}} - \tfrac{1}{2}\frac{\sqrt{\rho_2 a_2}}{\sqrt{\rho_3 a_3}}\right) \\
&\qquad \cos\left(\left[\frac{L_1}{c_1} + \frac{L_2}{c_2} - \frac{L_3}{c_3}\right]\omega\right) \textit{(third harmonic)} \\
&+ \tfrac{1}{4}\left(1 - \tfrac{1}{2}\frac{\sqrt{\rho_1 a_1}}{\sqrt{\rho_2 a_2}} - \tfrac{1}{2}\frac{\sqrt{\rho_1 a_1}}{\sqrt{\rho_3 a_3}} + \tfrac{1}{2}\frac{\sqrt{\rho_2 a_2}}{\sqrt{\rho_3 a_3}}\right) \\
&\qquad \cos\left(\left[\frac{L_1}{c_1} - \frac{L_2}{c_2} - \frac{L_3}{c_3}\right]\omega\right) \textit{.(fourth harmonic)}
\end{aligned} \tag{18}$$

The design proposed in Figure 8 achieves the goals we set up before. Figure 9 displays the equivalent dispersion relation in the right panel and, more importantly, the spectrum we envisioned in the left one.

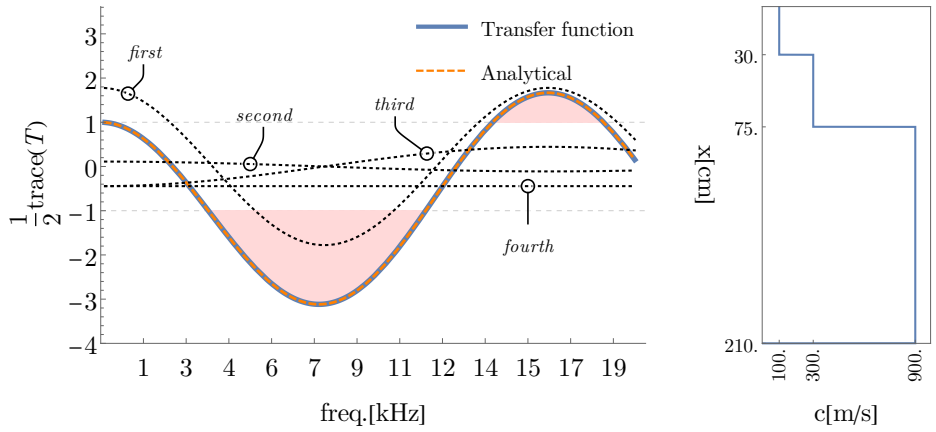

FIGURE 8. Profile designed (right panel) and half-trace function (left panel) with corresponding shaded regions corresponding to bandgaps; the harmonics are marked with dotted lines and called by their order (see section 4).

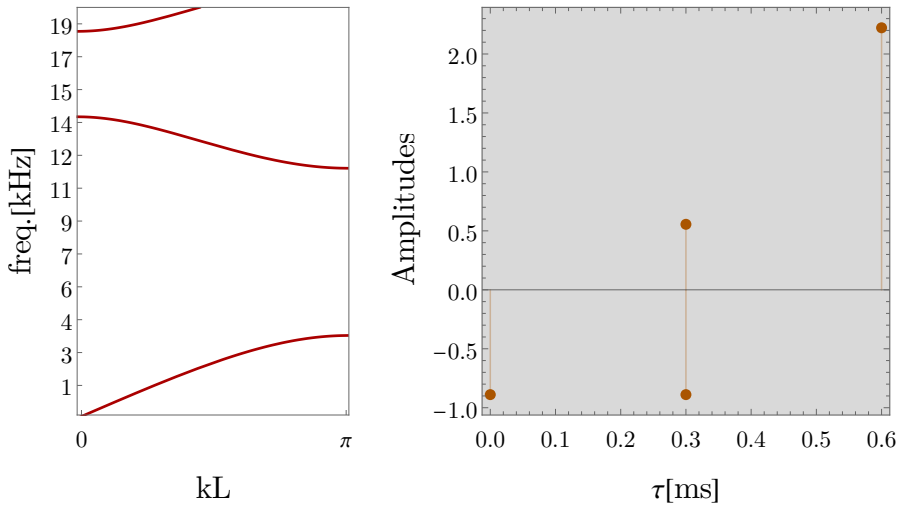

FIGURE 9. Dispersion relation diagram (left panel) and one-sided spectrum (right panel) of the design in Figure 9.

Gazing at Figure 4, one can see that we could do even better: the approach would consist of having many "slow" harmonics with large negative amplitude and many "quick" harmonics with large positive amplitude, while making sure that the amplitude of intermediate harmonics remains relatively small. As a matter of fact, Figure 5 displays just that: out of 8 harmonics, the two lowest ones have negative amplitude much greater than the next five ones, and the eighth and last one does possess positive amplitude greater than the 5 previous ones and of the same order as the two slowest ones.

Equally compelling is extending the comparison to the profile in Figure 6, which may, at first glance, appear similar to the one in Figure 4: the profiles may resemble each other but, in terms of spectra, they are very different: while in Figure 4 the largest amplitudes are exactly where they should be to maximize the bandgap, quite the opposite happens in Figure 6, i.e. smaller amplitudes at the border of the spectrum and greater ones in the inner range.

From the prior considerations one can posit that an "ideal" spectrum (in the sense of lowest-frequency-bandgap maximization) would display a "S"-shaped distribution of amplitudes: large and negative at the lowest values and large and positive at the largest ones, while intermediate harmonics' amplitudes would be much smaller.

5. Final remarks and future work

It has been shown that the half-trace function that governs the dispersion relation in periodic layered media possesses neat spectral properties: namely, the one-sided spectrum is made up by 2^{N-1} distinct harmonics, whose period is independent of

the order of the layering, but whose amplitudes and phase delay do depend on the disposition of the layers. We have also shown that the phase delay between harmonics is either 0 or π radians, and that the dispersion relation of the laminate can be constructed using combinatorics expressed by multi-indices. As mentioned repeatedly, the spectrum of the half-trace not only unveils a new understanding of the dispersion relation features, it also can serve as an innovatory design tool. In the Section 4 we showcased how the first gap can be optimized employing spectral arguments. The spectrum of the half-trace may be the means to unveil all the design possibilities when it comes to engineering dispersion relations in layered media.

When it comes to future contributions in the more theoretical aspects, it seems paramount to obtain a satisfactory mathematical explanation of the underlying structure of the problem. For instance, there better be a good reason justifying the hefty presence of combinatorics (multi-indices). The answer to this and similar questions must come necessarily from Group Theory. A deeper appraisal of the mathematical structure of the phenomenon, beyond its purely theoretical interest, could provide compelling answers as to the design space.

The many branches of Physics and Engineering where the transfer matrix method finds application could benefit from the knowledge of the spectrum of the half-trace function, or, more generally, of the spectral properties of cumulative transfer matrices/propagators.

In the realm of metamaterials, the dispersion relation of electromagnetic and acoustic waves can be engineered as well. In Optics, certain entries of the global propagator can be related to the reflectivity of the layering, so optimizing in terms of spectrum would also be possible there.

There are many other applications in the linear-elastic quarter beyond dispersion relations. Seismology applications were mentioned in Section 1, so let us delve on the two wave propagation scenarios whose transfer matrices are two-by-two matrices:

- Inclined SH-wave systems: to consider this scenario we would have to qualitatively modify one entry of the propagator matrix in order to introduce the ray parameter p [7]; see that the governing vector ODE, recall eq. (3), in this case is

$$\frac{d}{dz}\begin{bmatrix}\hat{u}_y\\ \tau_{yz}\end{bmatrix} = \begin{bmatrix}0 & 1/\mu\\ \omega^2(\mu p^2-\rho) & 0\end{bmatrix}\begin{bmatrix}\hat{u}_y\\ \tau_{yz}\end{bmatrix} = \boldsymbol{A}\boldsymbol{f}(z)\,, \tag{19}$$

  where ρ and μ are the density and shear modulus of the material conforming the layer, and $p = \sin(\gamma)/\sqrt{\mu/\rho}$, where γ is the inclination angle with respect to the normal at the interface. See that now $\boldsymbol{A}$ can be rank-deficient: even though still $\operatorname{trace}(\boldsymbol{A}) = 0$, the determinant of the layer matrix can equal zero, unlike in the previous case or for SH waves impinging normally to the interfaces ($\gamma = 0$). The latter happens precisely when ray arrived in the layer at the critical angle. Let us also mention that the propagation of inclined electromagnetic and acoustic waves obeys a similar formalism.
- Love waves: likewise, for this kind of surface wave [7], relevant displacement and stresses can be written as $u_y = l_1(\mathrm{k}, z, \omega)e^{\mathrm{i}(\mathrm{k}x-\omega t)}$, $\tau_{yz} = l_2(\mathrm{k}, z, \omega)e^{\mathrm{i}(\mathrm{k}x-\omega t)}$, $\tau_{xy} = \mathrm{i}\mathrm{k}l_1(\mathrm{k}, z, \omega)e^{\mathrm{i}(\mathrm{k}x-\omega t)}$, and the equivalent of eq. (3) is therefore

$$\frac{d}{dz}\begin{bmatrix}l_1\\ l_2\end{bmatrix} = \begin{bmatrix}0 & 1/\mu\\ \mu\mathrm{k}^2-\rho\omega^2 & 0\end{bmatrix}\begin{bmatrix}\hat{u}\\ \hat{\tau}_{xz}\end{bmatrix} = \boldsymbol{A}\boldsymbol{f}(z)\,. \tag{20}$$

The determinant of the layer matrix goes one step beyond now: it can take any real value, including negative ones. As a consequence of this, the entries of the elementary transfer matrix for a given layer can take complex values (as they are proportional to the square root of the aforementioned determinant), what means that one would have to examine the group $SL(2,\mathbb{C})$ in lieu of $SL(2,\mathbb{R})$. $SL(2,\mathbb{C})$ must, in some theoretical way, govern the dispersion relation of Love waves in layered media. Another distinct and interesting feature of considering surface waves in general is that two boundary conditions, (a) stress-free surface and (b) vanishing at infinite depth, replace periodicity conditions.

There are other applications in Seismology, inclined P-SV wave systems and surface Rayleigh waves, but require four-by-four matrices, and they seem hence more difficult to tackle.

Supplementary Material

A *Mathematica* notebook [26] containing the computations leading to results (including figures) shown in the text can be found in the repository named `spectrum_trace` in the author's GitHub page `github.com/jgarciasuarez`.

References

[1] John Lekner. Light in periodically stratified media. *JOSA A*, 11(11):2892–2899, 1994.

[2] Mahito Kohmoto, Leo P Kadanoff, and Chao Tang. Localization problem in one dimension: Mapping and escape. *Physical Review Letters*, 50(23):1870, 1983.

[3] Mahito Kohmoto, Bill Sutherland, and K Iguchi. Localization of optics: Quasiperiodic media. *Physical review letters*, 58(23):2436, 1987.

[4] Enrique Maciá. Hierarchical description of phonon dynamics on finite fibonacci superlattices. *Physical review B*, 73(18):184303, 2006.

[5] David Damanik, Anton Gorodetski, and William Yessen. The fibonacci hamiltonian. *Inventiones mathematicae*, 206(3):629–692, 2016.

[6] Mingrong Shen and Wenwu Cao. Acoustic bandgap formation in a periodic structure with multilayer unit cells. *Journal of Physics D: Applied Physics*, 33(10):1150, 2000.

[7] Keiiti Aki and Paul G Richards. *Quantitative seismology*. 2002.

[8] Ari Ben-Menahem and Sarva Jit Singh. *Seismic waves and sources*. Springer Science & Business Media, 2012.

[9] Freeman Gilbert and George E Backus. Propagator matrices in elastic wave and vibration problems. *Geophysics*, 31(2):326–332, 1966.

[10] Gal Shmuel and Ram Band. Universality of the frequency spectrum of laminates. *Journal of the Mechanics and Physics of Solids*, 92:127–136, 2016.

[11] Ankit Srivastava. Metamaterial properties of periodic laminates. *Journal of the Mechanics and Physics of Solids*, 96:252–263, 2016.

[12] John R Willis. Negative refraction in a laminate. *Journal of the Mechanics and Physics of Solids*, 97:10–18, 2016.

[13] Lorenzo Morini and Massimiliano Gei. Waves in one-dimensional quasicrystalline structures: dynamical trace mapping, scaling and self-similarity of the spectrum. *Journal of the Mechanics and Physics of Solids*, 119:83–103, 2018.

[14] Lorenzo Morini, Zafar Gokay Tetik, Gal Shmuel, and Massimiliano Gei. On the universality of the frequency spectrum and band-gap optimization of quasicrystalline-generated structured rods. *Philosophical Transactions of the Royal Society A*, 378(2162):20190240, 2020.

[15] Mahmoud I. Hussein, Michael J. Leamy, and Massimo Ruzzene. Dynamics of Phononic Materials and Structures: Historical Origins, Recent Progress, and Future Outlook. *Applied Mechanics Reviews*, 66(4), 05 2014. 040802.

[16] Ben Lustig and Gal Shmuel. On the band gap universality of multiphase laminates and its applications. *Journal of the Mechanics and Physics of Solids*, 117:37–53, 2018.

[17] Gal Shmuel and Ram Band. Universality of the frequency spectrum of laminates. *Journal of the Mechanics and Physics of Solids*, 92:127–136, 2016.

[18] Witarto Witarto, Kalyana B Nakshatrala, and Yi-Lung Mo. Global sensitivity analysis of frequency band gaps in one-dimensional phononic crystals. *Mechanics of Materials*, 134:38–53, 2019.

[19] Xinnan Liu, Yiqiang Ren, Xiaoruan Song, and W Witarto. A global sensitivity analysis method based on the gauss-lobatto integration and its application in layered periodic foundations with initial stress. *Composite Structures*, 244:112297, 2020.

[20] Brian Hall. *Lie groups, Lie algebras, and representations: an elementary introduction*, volume 222. Springer, 2015.

[21] Marcel Novaes. Some basics of su (1, 1). *Revista Brasileira de Ensino de Fisica*, 26(4):351–357, 2004.

[22] Charles Kittel, Paul McEuen, and Paul McEuen. *Introduction to solid state physics*, volume 8. Wiley New York, 1996.

[23] Lawrence C. Evans. *Partial differential equations*. American Mathematical Society, Providence, R.I., 2010.

[24] James Kaklamanos, Laurie G Baise, Eric M Thompson, and Luis Dorfmann. Comparison of 1d linear, equivalent-linear, and nonlinear site response models at six kik-net validation sites. *Soil Dynamics and Earthquake Engineering*, 69:207–219, 2015.

[25] Yoshimitsu Okada, Keiji Kasahara, Sadaki Hori, Kazushige Obara, Shoji Sekiguchi, Hiroyuki Fujiwara, and Akira Yamamoto. Recent progress of seismic observation networks in japan—hi-net, f-net, k-net and kik-net—. *Earth, Planets and Space*, 56(8):xv–xxviii, 2004.

[26] Stephen Wolfram. *The mathematica book*, volume 4. Cambridge University Press Cambridge, 2000.

Appendix A. Derivation of exact general expressions

A.1. **Review of multi-index notation.** A binary multi-index $\mathsf{b} \in (\{0,\,1\})^N$ is an N-tuple of numbers, in this case being either 0 or 1. Its "degree" is equal to $|\mathsf{b}| = \mathsf{b}_1 + \ldots + \mathsf{b}_N$, thus, in this case, the degree is equal to the number of non-zero elements.

When a variable, call it $x \in \mathbb{R}^N$, is raised to the multi-index yields

$$x^{\mathsf{b}} = x_1^{\mathsf{b}_1} \ldots x_N^{\mathsf{b}_N}\,. \tag{21}$$

Note that a certain polynomial of degree N, $p(x) \in \mathbb{P}_N(\mathbb{R})$, can be written as

$$p(x) = \sum_{\beta=0}^{\lfloor N/2 \rfloor} \sum_{|\mathsf{b}|=2\beta} C_{\mathsf{b}} x^{\mathsf{b}}\,. \tag{22}$$

So, for instance, if $N = 3$:

$$\text{for } |\mathsf{b}| = 0 : \{x_1^0 x_2^0 x_3^0\} = \{1\}\,, \tag{23a}$$

$$\text{for } |\mathsf{b}| = 2 : \{x_1^1 x_2^1 x_3^0,\, x_1^1 x_2^0 x_3^1,\, x_1^0 x_2^1 x_3^1\} = \{x_1x_2,\, x_1x_3,\, x_2x_3\}\,, \tag{23b}$$

hence, it defines the following polynomial:

$$p(x) = \sum_{\beta=0}^{1} \sum_{|\mathsf{b}|=2\beta} C_{\mathsf{b}} x^{\mathsf{b}} = C_{(0,0,0)} + C_{(1,1,0)} x_1x_2 + C_{(1,0,1)} x_1x_3 + C_{(0,1,1)} x_2x_3\,. \tag{24}$$

Yet another example, if $N = 4$:

$$\text{for } |\mathsf{b}| = 0 : \{x_1^0 x_2^0 x_3^0 x_4^0\} = \{1\}\,, \tag{25}$$

$$\begin{aligned}\text{for } |\mathsf{b}| = 2 : \{&x_1^1 x_2^1 x_3^0 x_4^0,\, x_1^1 x_2^0 x_3^1 x_4^0,\, x_1^1 x_2^0 x_3^0 x_4^1,\, x_1^0 x_2^1 x_3^1 x_4^0,\, x_1^0 x_2^1 x_3^0 x_4^1,\, x_1^0 x_2^0 x_3^1 x_4^1\} \\ &= \{x_1x_2,\, x_1x_3,\, x_1x_4,\, x_2x_3,\, x_2x_4,\, x_3x_4\}\,,\end{aligned} \tag{26}$$

$$\text{for } |\mathsf{b}| = 4 : \{x_1^1 x_2^1 x_3^1 x_4^1\} = \{x_1x_2x_3x_4\}\,, \tag{27}$$

and thus

$$\begin{aligned}p(x) = \sum_{\beta=0}^{2} \sum_{|\mathsf{b}|=2\beta} C_{\mathsf{b}} x^{\mathsf{b}} = {} & C_{(0,0,0,0)} + C_{(1,1,0,0)} x_1x_2 + C_{(1,0,1,0)} x_1x_3 + C_{(1,0,0,1)} x_1x_4 \\ & + C_{(0,1,1,0)} x_2x_3 + C_{(0,1,0,1)} x_2x_4 + C_{(0,0,1,1)} x_3x_4 + C_{(1,1,1,1)} x_1x_2x_3x_4\,.\end{aligned} \tag{28}$$

A.2. **Dimensionless form of the matrix system.** Again, consider a N-layer cell; assume different lengths L_i, $i = 1, \ldots, N$. The total length of the cell is therefore $L = \sum_{i=1}^{N} L_i$.

Define a characteristic displacement $\mathcal{U}$, and a characteristic force $\sigma_{ch} = a_{ch} \cdot \mathcal{U}/L$, where the value of a_{ch} can be thought to be the one of any of the layers. The longitudinal coordinate within the layer is parametrized using $\xi = x/L$. Using these new parameters, eq. (3) can be rewritten as

$$\frac{d\tilde{\boldsymbol{f}}}{d\xi} = \frac{d}{d\xi}\begin{bmatrix}\tilde{u} \\ \tilde{\sigma}\end{bmatrix} = \begin{bmatrix}0 & 1/\gamma_k \\ -\eta_k r^2 & 0\end{bmatrix}\begin{bmatrix}\tilde{u} \\ \tilde{\sigma}\end{bmatrix} = \boldsymbol{A}_k \tilde{\boldsymbol{f}}(\xi)\,, \tag{29}$$

where $\tilde{u} = \hat{u}/\mathcal{U}$, $\tilde{\sigma} = \hat{\sigma}A/\sigma_{ch}$, and $\eta_k = \rho_k/\rho_{ch}$, $r = \omega L/\sqrt{a_{ch}/\rho_{ch}}$.

At the bottom of the k-th layer, wherein $\xi - \xi_{ref} = \beta_k = L_k/L$,

$$\tilde{\boldsymbol{f}}(\xi_k) = \exp\left(\begin{bmatrix} 0 & \beta_k/\gamma_k \\ -\beta_k\eta_k r^2 & 0 \end{bmatrix}\right)\tilde{\boldsymbol{f}}(\xi_{k-1}) \tag{30a}$$

$$= \exp\left(\begin{bmatrix} 0 & \alpha_k \\ \alpha_k R_k^2 & 0 \end{bmatrix}\right)\tilde{\boldsymbol{f}}(\xi_{k-1}) \tag{30b}$$

$$= \begin{bmatrix} \cosh(\alpha_k R_k) & R_k^{-1}\sinh(\alpha_k R_k) \\ R_k\,\sinh(\alpha_k R_k) & \cosh(\alpha_k R_k) \end{bmatrix}\tilde{\boldsymbol{f}}(\xi_{k-1})\,, \tag{30c}$$

where $\alpha_k = \beta_k/\gamma_k$, $\sinh(\alpha_k R_k) = \mathrm{i}\sin(r_k)$ and $\cosh(\alpha_k R_k) = \cos(r_k)$, where $r_k = \omega h_k/\sqrt{\mu_k/\rho_k}$, and $R_k = r\sqrt{-\gamma_k\eta_k} = r\sqrt{-\rho_k\mu_k/\rho_{ch}a_{ch}}$.

A.3. **Analogy with Lorentz transformations.** Compare the last expression to the Lorentz transformation realized with a 2x2 matrix of a "boost" of magnitude τ_0 along the direction ϕ_0, $\mathrm{T}_{\tau_0,\phi_0}$ [21],

$$\mathrm{T}_{\tau_0,\phi_0} = \begin{bmatrix} \cosh(\tau_0/2) & e^{-\mathrm{i}\phi_0}\sinh(\tau_0/2) \\ e^{\mathrm{i}\phi_0}\sinh(\tau_0/2) & \cosh(\tau_0/2) \end{bmatrix}. \tag{31}$$

We will use an analogy to this type of transformations as stepping stone to understand the action of the transfer matrices.

The superposition of any number of layers can be seen as a composition of any number of successive Lorentz boosts. It is a well-known fact that the composition of boosts is not a boost, but a composition of a rotation and a boost [21]; this can be regarded as a re-statement of a well-known result in Homogeneization Theory [see *D. Cioranescu, and P. Donato. An introduction to homogenization. Vol. 17. Oxford: Oxford University Press, 1999*]: a set of continuum layers cannot be homogeneized into a single equivalent layer for the purpose of arbitrary-wavelength wave propagation (such homogeneization is only feasible in the limit of small wavelengths, see the reference for more details).

In any case, the boost can be represented by matrices of the type

$$\begin{bmatrix} \zeta_1 & \bar{\zeta}_2 \\ \zeta_2 & \bar{\zeta}_1 \end{bmatrix}, \tag{32}$$

where $\bar{\cdot}$ amounts to the conjugation. If we move to projective coordinates (hence we can re-scale the entries of the matrix freely as long as all of them are scaled by the same factor) the action over a vector can be thus realized by means of fractional transformations, i.e., given an starting element z, the new element, according to the transformation defined by eq. (32), z' is

$$z' = \frac{\zeta_1 z + \zeta_2}{\bar{\zeta}_2 z + \bar{\zeta}_1}, \tag{33}$$

which, in the matrix form is expressed as

$$[z, 1]^\top \begin{bmatrix} \zeta_1 & \bar{\zeta}_2 \\ \zeta_2 & \bar{\zeta}_1 \end{bmatrix}, \tag{34}$$

the term 1 actually gives away that we pass to work over the projective line. See that if all the entries of the boost matrix are multiplied by the same factor, the

transformation does not change eq. (33). The expression of the boost in projective coordinates is therefore

$$\mathrm{T}_{\tau_0,\phi_0}(\zeta) = \frac{(\cosh\tau_0/2)\zeta + e^{\mathrm{i}\phi_0}\sinh\tau_0/2}{(e^{-\mathrm{i}\phi_0}\sinh\tau_0/2)\zeta + \cosh\tau_0/2}\,. \tag{35}$$

See how, in general, these transformations are not commutative (the order in which successive transformations are effectuated is critical to the final result).

Pushing the analogy, we claim that eq. (30), up to scaling by a constant, can be expressed as

$$\tilde{\boldsymbol{f}}(\xi_k) = \frac{\cosh(\alpha_k R_k)\tilde{\boldsymbol{f}}(\xi_{k-1}) + R_k\,\sinh(\alpha_k R_k)}{R_k^{-1}\sinh(\alpha_k R_k)\tilde{\boldsymbol{f}}(\xi_{k-1}) + \cosh(\alpha_k R_k)} = \frac{\tilde{\boldsymbol{f}}(\xi_{k-1}) + R_k\,\tanh(\alpha_k R_k)}{R_k^{-1}\tanh(\alpha_k R_k)\tilde{\boldsymbol{f}}(\xi_{k-1}) + 1}\,, \tag{36}$$

wherein, abusing the notation, now $\tilde{\boldsymbol{f}}$ is understood as a complex number. As we wish to find a recursion formula when combining N successive boosts, let us put the previous formula in a more compact form:

$$\tilde{\boldsymbol{f}}(\xi_k) = \frac{c_k\tilde{\boldsymbol{f}}(\xi_{k-1}) + s_k}{s_k^*\tilde{\boldsymbol{f}}(\xi_{k-1}) + c_k^*}\,, \tag{37}$$

wherein the asterisk indicates that the tanh term is *divided* by the corresponding R_k. The asterisk is also added to the other term to facilitate appraising the recursion, it is understood to change nothing in that case.

A.4. **Obtaining the general recursion of the cumulative transfer matrix.**

A.4.1. *Particular case: one-layer system.* In this case, simply use eq. (37):

$$\boldsymbol{f}(1) = \frac{c_1\boldsymbol{f}(0) + s_1}{s_1^*\boldsymbol{f}(0) + c_1^*} \tag{38a}$$

$$= \frac{\cos(r_1)\boldsymbol{f}(0) + \sqrt{-\rho_1 a_1/\rho_{ch}a_{ch}}\mathrm{i}\sin(r_1)}{\frac{\mathrm{i}\sin(r_1)}{\sqrt{-\rho_1 a_1/\rho_{ch}a_{ch}}\mathrm{i}}\boldsymbol{f}(0) + \cos(r_1)} \tag{38b}$$

$$= \frac{\boldsymbol{f}(0) - \sqrt{\frac{\rho_1 a_1}{\rho_{ch}a_{ch}}}\tan(r_1)}{\sqrt{\frac{\rho_{ch}a_{ch}}{\rho_1 a_1}}\tan(r_1)\boldsymbol{f}(0) + 1}\,, \tag{38c}$$

thus we can state also

$$c_1 = c_1^* = 1\,, \tag{39a}$$

$$s_1 = -\sqrt{\frac{\rho_1 a_1}{\rho_{ch}a_{ch}}}\tan(r_1)\,, \tag{39b}$$

$$s_1^* = \sqrt{\frac{\rho_{ch}a_{ch}}{\rho_1 a_1}}\tan(r_1) \tag{39c}$$

Hence, after scaling back by the cosine, in the simplest case we obtain

$$\frac{1}{2}\mathrm{trace}(\boldsymbol{T}) = \frac{1}{2}\cos\left(\frac{\omega h_1}{a_1}\right)(c_1 + c_1^*) = \cos\left(\frac{\omega L_1}{a_1}\right)\,, \tag{40}$$

which means that the dispersion relation in a homogeneous layer presents no bandgaps.

A.4.2. *Particular case: two-layer system.* Perform two subsequent fractional transformations in this case,

$$\boldsymbol{f}(\beta_1+\beta_2)=\boldsymbol{f}(1)=\frac{c_2\boldsymbol{f}(\beta_1)+s_2}{s_2^*\boldsymbol{f}(\beta_1)+c_2^*}=\frac{c_2\frac{c_1\boldsymbol{f}(0)+s_1}{s_1^*\boldsymbol{f}(0)+c_1^*}+s_2}{s_2^*\frac{c_1\boldsymbol{f}(0)+s_1}{s_1^*\boldsymbol{f}(0)+c_1^*}+c_2^*} \tag{41a}$$

$$=\frac{(c_2c_1+s_2s_1^*)\boldsymbol{f}(0)+(s_2c_1^*+c_2s_1)}{(s_2^*c_1+c_2^*s_1^*)\boldsymbol{f}(0)+(c_2^*c_1^*+s_2^*s_1)}\,, \tag{41b}$$

then, scaling back multiplying by two cosines,

$$\frac{1}{2}\text{trace}(\boldsymbol{T})=\frac{1}{2}\cos\left(\frac{\omega L_1}{a_1}\right)\cos\left(\frac{\omega L_1}{a_2}\right)\left[(c_2c_1+s_2s_1^*)+(c_2^*c_1^*+s_2^*s_1)\right]\,, \tag{42a}$$

For the purpose of easing notation as we push the recurrence forward, let us call

$$c_{2,1}=c_2c_1+s_2s_1^*=1-\sqrt{\frac{\rho_1a_1}{\rho_2a_2}}\tan(r_1)\tan(r_2)\,, \tag{43}$$

$$c_{2,1}^*=c_2^*c_1^*+s_2^*s_1=1-\sqrt{\frac{\rho_2a_2}{\rho_1a_1}}\tan(r_1)\tan(r_2)\,, \tag{44}$$

$$s_{2,1}=s_2c_1^*+c_2s_1=-\sqrt{\frac{\rho_2\mu_2}{\rho_{ch}a_{ch}}}\tan(r_2)-\sqrt{\frac{\rho_1a_1}{\rho_{ch}a_{ch}}}\tan(r_1)\,, \tag{45}$$

$$s_{2,1}^*=s_2^*c_1+c_2^*s_1^*=\sqrt{\frac{\rho_{ch}a_{ch}}{\rho_2a_2}}\tan(r_2)+\sqrt{\frac{\rho_{ch}a_{ch}}{\rho_1a_1}}\tan(r_1)\,, \tag{46}$$

see how the "c-terms" accumulate two tangent factors in one addend at once while the "s-terms" contain two terms with one tangent each. This structure persists as more layers are stacked.

A.4.3. $N>2$ *number of layers.* For the general case, just set a recurrence up:

$$c_{i,1}=c_ic_{i-1,1}+s_is_{i-1,1}^*\,, \tag{47a}$$

$$c_{i,1}^*=c_i^*c_{i-1,1}^*+s_i^*s_{i-1,1}\,, \tag{47b}$$

$$s_{i,1}=s_ic_{i-1,1}^*+c_i^*s_{i-1,1}\,, \tag{47c}$$

$$s_{i,1}^*=s_i^*c_{i-1,1}+c_is_{i-1,1}^*\,, \tag{47d}$$

and proceed to "unzip" it to see that (the scaling-back by the cosines already included)

$$c_{1,N}=\left(\prod_{i=1}^{N}\cos(r_i)\right)\left(\sum_{\beta=0}^{\lfloor N/2\rfloor}\sum_{|\mathsf{b}|=2\beta}K_{\mathsf{b}}\tan(r)^{\mathsf{b}}\right)\,, \tag{48a}$$

$$s_{1,N}=\omega\left(\prod_{i=1}^{N}\cos(r_i)\right)\left(\sum_{\beta=0}^{\lfloor\frac{N-1}{2}\rfloor}\sum_{|\mathsf{b}|=1+2\beta}H_{\mathsf{b}}\tan(r)^{\mathsf{b}}\right)\,, \tag{48b}$$

while the coefficients

$$K_{\mathsf{b}}=(-1)^{|\mathsf{b}|/2}(\sqrt{\rho\mu})^{\mathsf{b}}\,, \tag{49a}$$

$$H_{\mathsf{b}}=(-1)^{(|\mathsf{b}|-1)/2}(\sqrt{\rho\mu})^{\mathsf{b}'}\,, \tag{49b}$$

where b has been presented in the body of the text, b' has also the same structure as b, but, in this case, if a one-entry is enclosed by other ones, the exponent becomes -1.

The coefficients with asterisk are given by the same expression but inverting the rations forming the coefficients.

Appendix B. Extra figures for other rod profiles

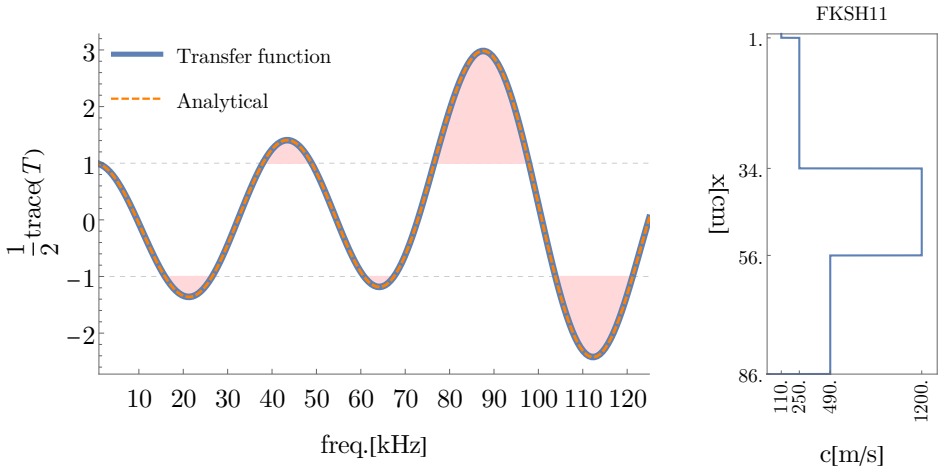

Figure 10. Dispersion diagram (left panel) and spectrum of half-trace (right panel) of rod having properties (right panel) that mirror Kik-Net site FKSH11.

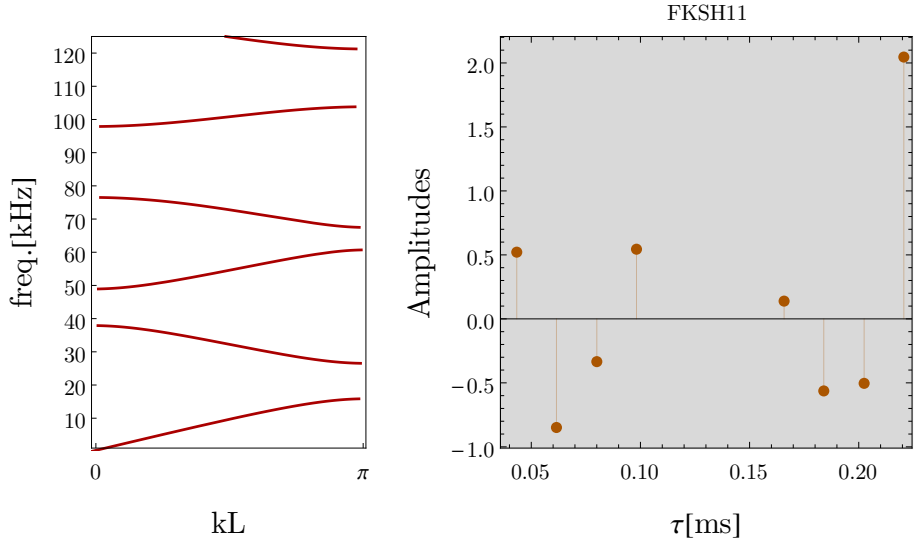

Figure 11. Dispersion diagram (left panel) and spectrum of half-trace (right panel) of rod having properties (right panel) that mirror Kik-Net site FKSH11.

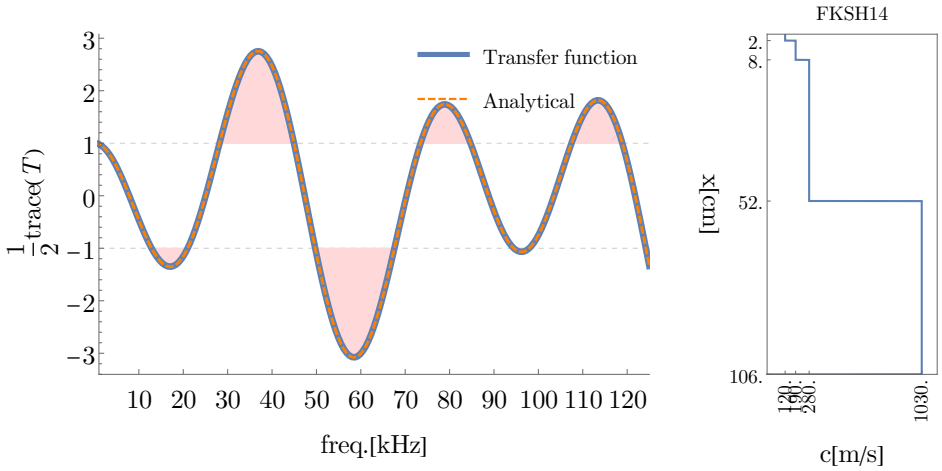

FIGURE 12. Dispersion diagram (left panel) and spectrum of half-trace (right panel) of rod having properties (right panel) that mirror Kik-Net site FHSK14.

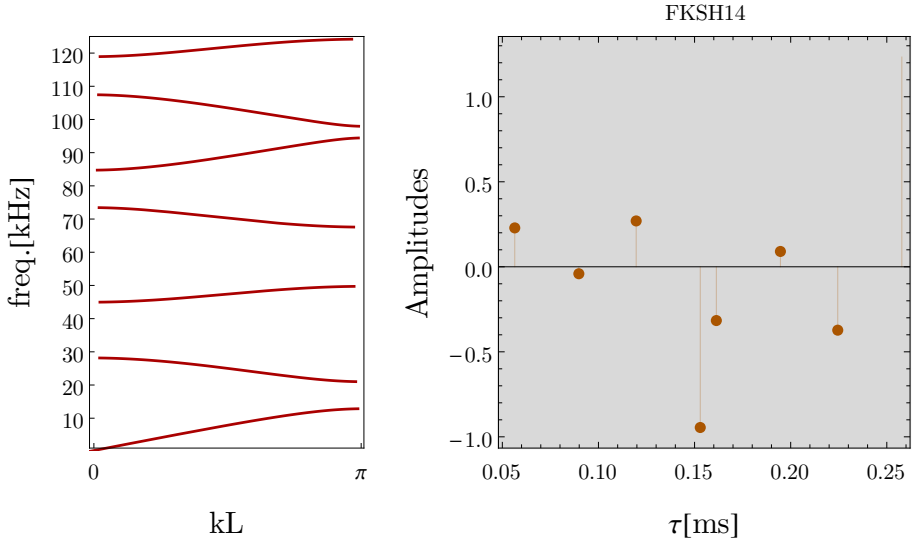

FIGURE 13. Dispersion diagram (left panel) and spectrum of half-trace (right panel) of rod having properties (right panel) that mirror Kik-Net site FHSK14.

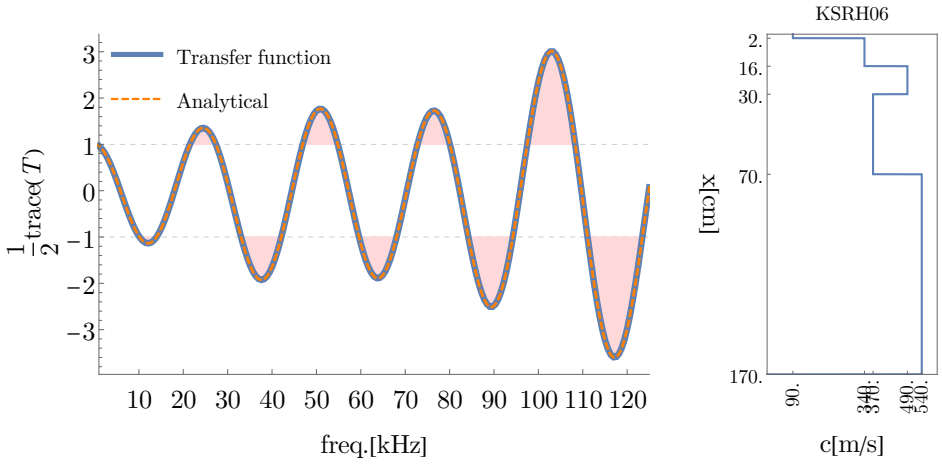

FIGURE 14. Dispersion diagram (left panel) and spectrum of half-trace (right panel) of rod having properties (right panel) that mirror Kik-Net site KSRH06.

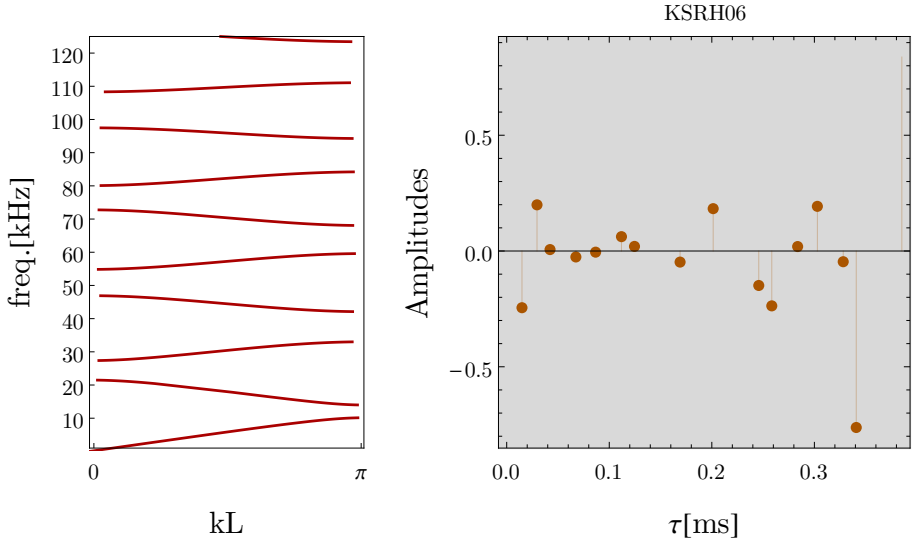

FIGURE 15. Dispersion diagram (left panel) and spectrum of half-trace (right panel) of rod having properties (right panel) that mirror Kik-Net site KSRH06.

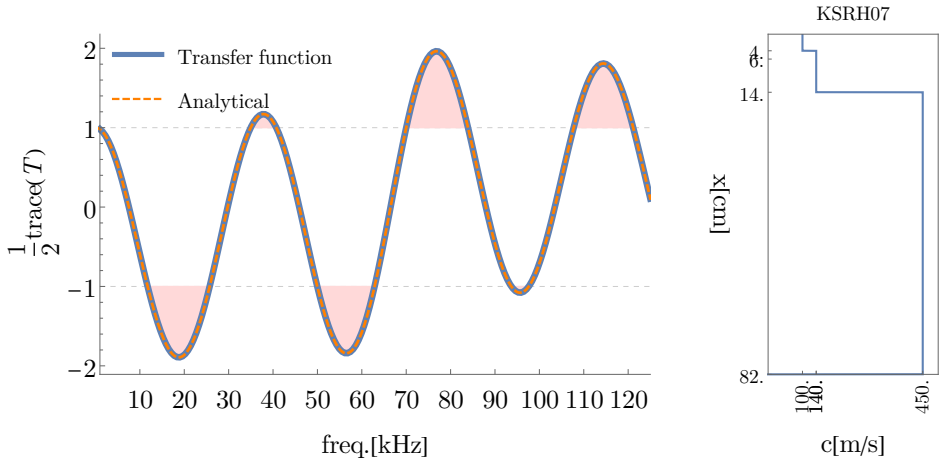

FIGURE 16. Dispersion diagram (left panel) and spectrum of half-trace (right panel) of rod having properties (right panel) that mirror Kik-Net site KSRH07.

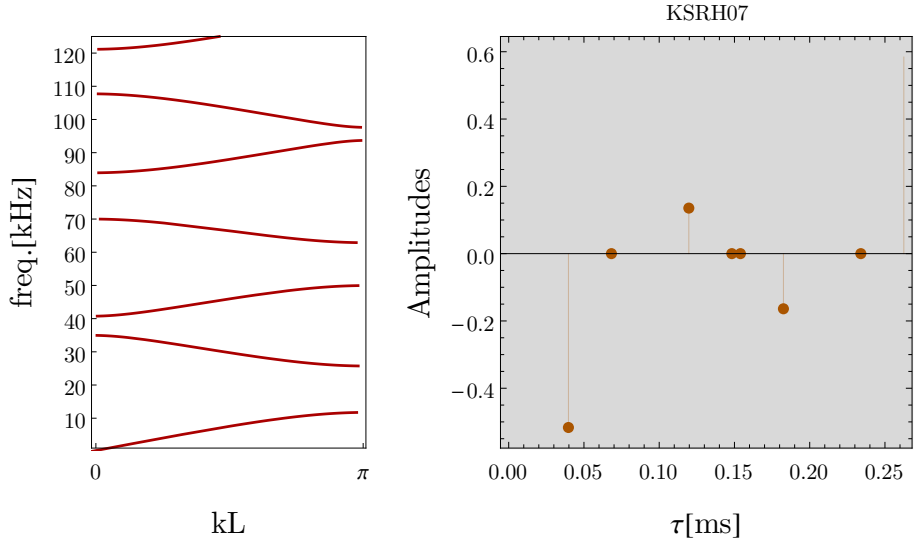

FIGURE 17. Dispersion diagram (left panel) and spectrum of half-trace (right panel) of rod having properties (right panel) that mirror Kik-Net site KSRH07.

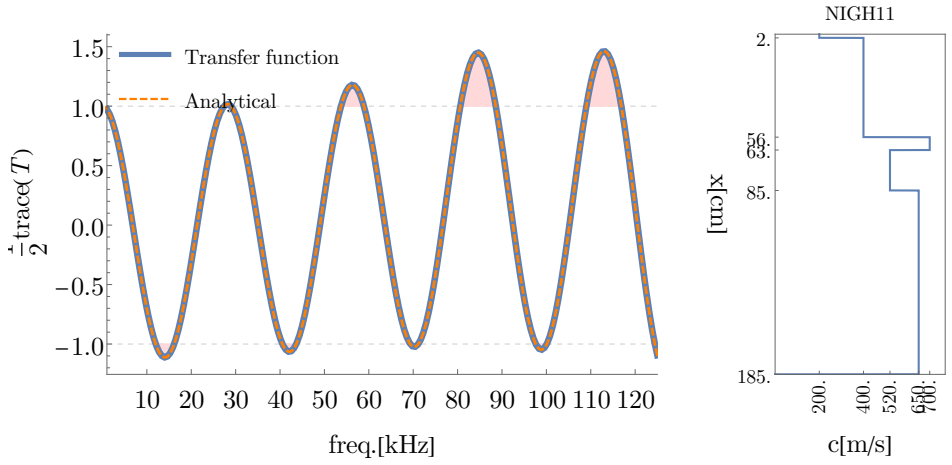

FIGURE 18. Dispersion diagram (left panel) and spectrum of half-trace (right panel) of rod having properties (right panel) that mirror Kik-Net site NIGH11.

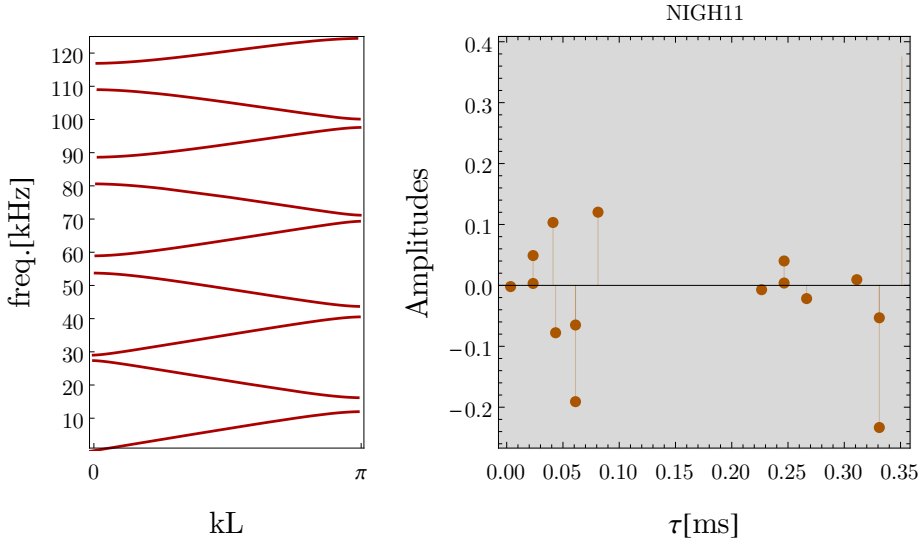

FIGURE 19. Dispersion diagram (left panel) and spectrum of half-trace (right panel) of rod having properties (right panel) that mirror Kik-Net site NIGH11.

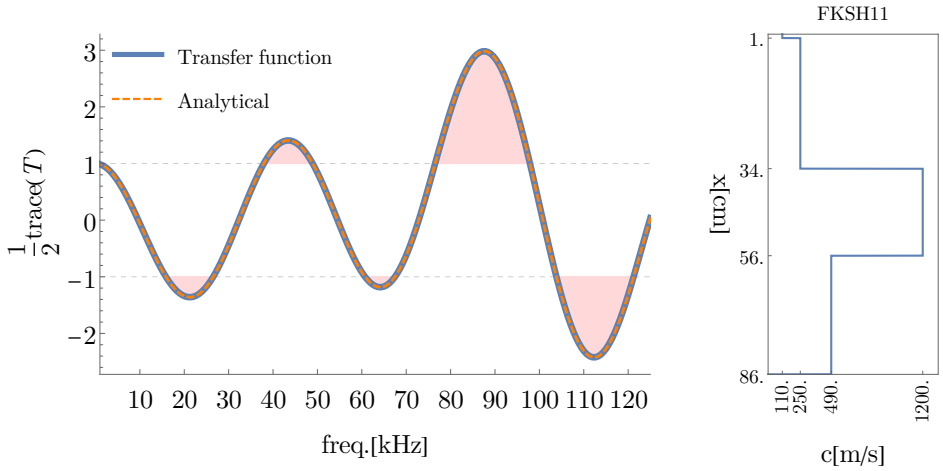

FIGURE 20. Dispersion diagram (left panel) and spectrum of half-trace (right panel) of rod having properties (right panel) that mirror Kik-Net site FKSH11.

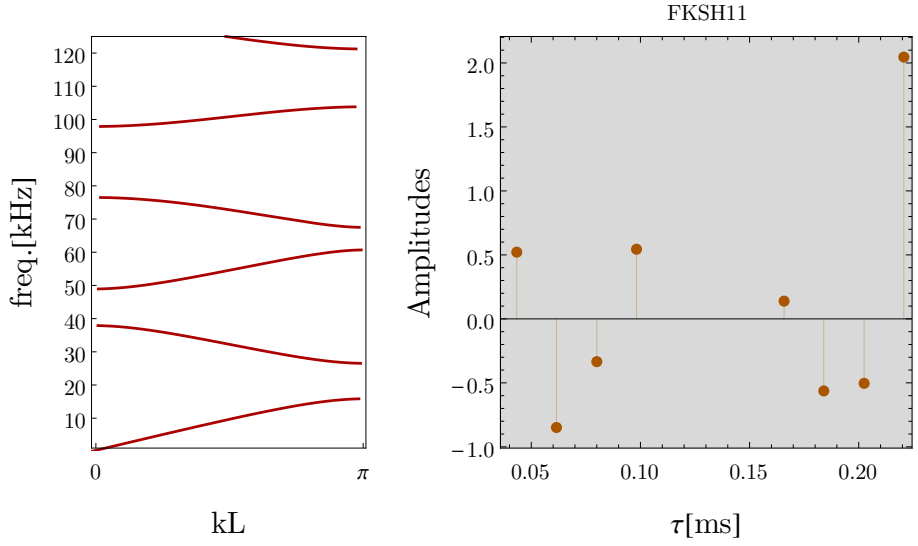

FIGURE 21. Dispersion diagram (left panel) and spectrum of half-trace (right panel) of rod having properties (right panel) that mirror Kik-Net site FKSH11.

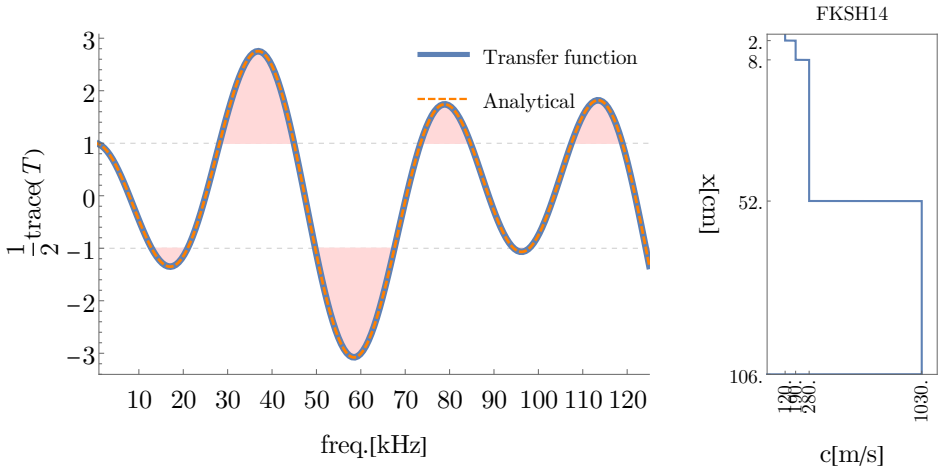

FIGURE 22. Dispersion diagram (left panel) and spectrum of half-trace (right panel) of rod having properties (right panel) that mirror Kik-Net site FHSK14.

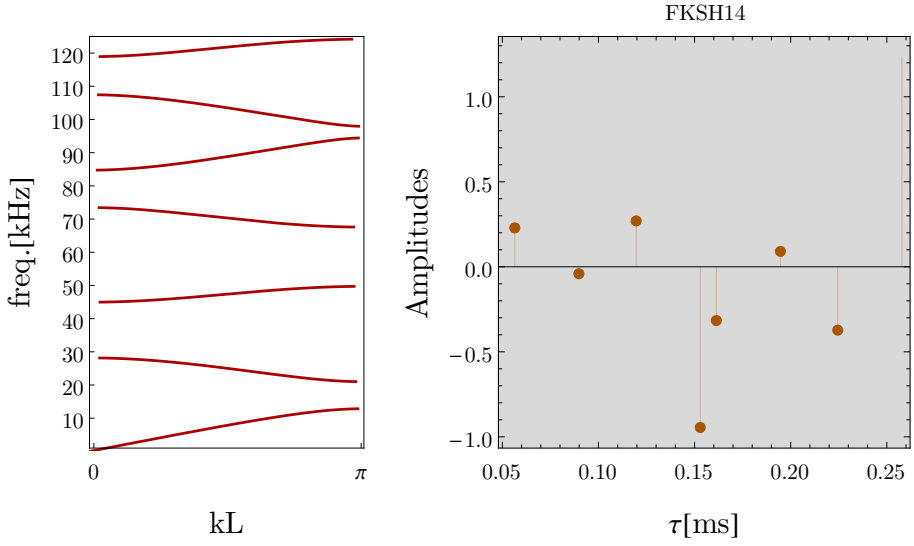

FIGURE 23. Dispersion diagram (left panel) and spectrum of half-trace (right panel) of rod having properties (right panel) that mirror Kik-Net site FHSK14.

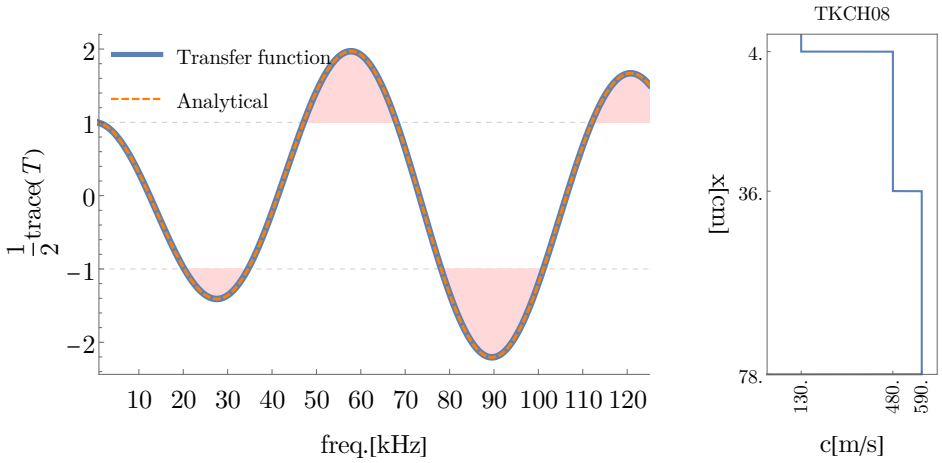

FIGURE 24. Dispersion diagram (left panel) and spectrum of half-trace (right panel) of rod having properties (right panel) that mirror Kik-Net site TKCH08.

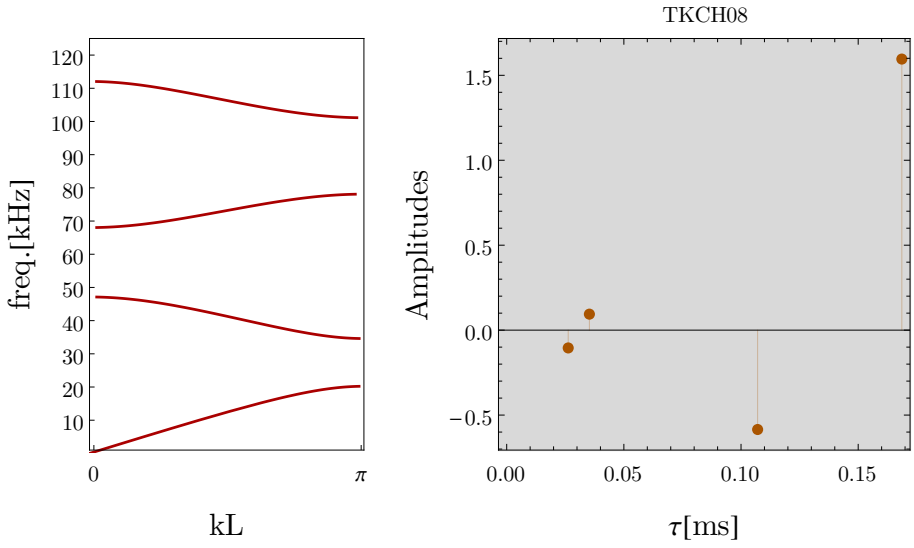

FIGURE 25. Dispersion diagram (left panel) and spectrum of half-trace (right panel) of rod having properties (right panel) that mirror Kik-Net site TKCH08.

Civil Engineering Institute École Politechnique Fédérale de Lausanne (EPFL), Lausanne, Switzerland
Email address: joaquin.garciasuarez@epfl.ch